Journal of Dentistry 71 (2018) 31–37

Contents lists available at ScienceDirect

Journal of Dentistry

journal homepage: www.elsevier.com/locate/jdent

Influence of the loci of non-cavitated fissure caries on its detection with optical coherence tomography

E. Zain[a], C.M. Zakian[b], H.P. Chew[a,*]

[a] Department of Restorative Dentistry, Faculty of Dentistry, University of Malaya, 50603, Kuala Lumpur, Malaysia
[b] R&D Department, Kevork Instruments, S.A. de C.V., 66450, San Nicolás de los Garza, N.L., Mexico

ARTICLE INFO

Keywords:
Caries detection
Non-cavitated fissure caries
Early occlusal caries
Optical coherence tomography
Sensitivity
Specificity

ABSTRACT

Objective: The main objective of this study was to evaluate the accuracy of optical coherence tomography (OCT) in detecting naturally occurring non-cavitated fissure caries (NCFC) in totality and at different loci by visually assessing cross-sectional OCT scans (B-scan) with an interpretation criterion. The secondary objective was to evaluate the agreement between dimensions of NCFC measured with OCT and polarized light microscopy (PLM).
Methods: 71 investigation sites of sound fissure and naturally occurring NCFC on human extracted premolars were identified and scanned with a swept-source OCT. The teeth were then sectioned bucco-lingually at the investigation sites and imaged using PLM. Two calibrated examiners trained on the B-scan NCFC visual interpretation criteria established for this study, assessed the investigation sites and results were validated against PLM.
Results: Detection sensitivity of B-scan for NCFC when fissures were assessed in totality, or on the slopes or walls separately are 0.98, 0.95, 0.94 and specificity are 0.95, 0.90, and 0.95. One-way ANOVA showed that width measurements of wall loci done with OCT and PLM were not statistically different. However, OCT height measurements of slope loci were statistically bigger with a constant bias of 0.08 mm (of which is not clinically significant) and OCT height measurements of wall loci were statistically smaller (0.57 mm) and Bland-Altman plots indicated presence of proportionate bias.
Conclusion: Visual assessment of B-scans with the interpretation criteria resulted in both high specificity and sensitivity and were not affected by loci location. OCT width measurement of wall loci is in agreement with PLM.
Clinical significance: Unanimous high sensitivity in this and previous studies indicate that visual assessment of B-scans reliably rule out NCFC. Detection accuracy was not affected by loci location. Width of wall loci and/or height of slope loci in OCT B-scan are to be used for monitoring NCFC but not height of wall loci.

1. Introduction

3.9 billion people are affected with oral conditions globally amongst which, untreated caries in permanent teeth is of the highest prevalence [1], with approximately 35.3 percent of adults suffering from this condition. Although occlusal surfaces represent only 13 percent of total surfaces of the permanent dentition [2], 88% of caries experienced by schoolchildren in the United States has been found to be pit and fissure lesions [3] and pit and fissures lesions had also been found to comprise the majority of the caries increment observed in both fluoridated and non-fluoridated communities [4]. Hence its prevention via fissure sealant in large scale public health effort had been advocated and carried out. Recent studies however had showed that unjudicial application of fissure sealant, especially in population with low caries risk does not increase the prevention potential of fissure sealant. Risk-adjusted remineralisation therapy for incipient fissure caries with fluoride, calcium-phosphate products and bioglass had been proposed and are being explored. Hence the detection and monitoring of progression of incipient lesions has become an integral part of modern caries management [5]. Incipient lesions had been defined as lesions with surface that appear macroscopically intact with no visual evidence of cavitation [6]. Such incipient lesions has also been referred to as non-cavitated caries lesions [7] and those along fissures can be termed as non-cavitated fissure caries (NCFC).

Visual inspection and radiography are the most ubiquitous methods used in the detection of fissure caries lesions clinically. Visual detection system such as the International Caries Detection and Assessment System (ICDAS) has been proven to have good accuracy and reproducibility [8,9]. However, such systems require training and calibration with a reference examiner [8–10] and can be time consuming [11]. It

* Corresponding author.
E-mail addresses: chewhp@um.edu.my, chewhp33@gmail.com (H.P. Chew).

https://doi.org/10.1016/j.jdent.2018.01.009
Received 19 October 2017; Received in revised form 9 January 2018; Accepted 23 January 2018

also falls short of true quantification as it uses qualitative assessment of features such as colour, texture and roughness. Radiograph has been proven to be useful in detecting occlusal fissure lesions that had extended into dentine. However, the sensitivity of detecting occlusal fissure lesions which is limited in enamel is low (0.14–0.38) [7,12]. Therefore, supplementary detection tools such as those based on laser fluorescence and electrical conductance had been explored and used for the detection of NCFC. However, they still lack either sensitivity or specificity [13].

Optical coherence tomography (OCT) is a method that can obtain cross-section images non-invasively, by measuring the backscattered intensity in depth of a specimen. Changes in the optical scattering properties of the enamel and dentine surfaces have been shown to occur when they are demineralised and a strong correlation between mineral loss and increased scattering coefficient have been observed [14,15]. This correlation of reflectivity and demineralisation has been used both qualitatively [16,17] and quantitatively [10,18] to either detect or quantify the severity and depth of a caries lesion. Quantitative methods attempt to use mathematical algorithm to automate analysis of the depth-profile of reflectivity (A-scans) for severity, depth and structural features of caries lesion. However, there are still challenges faced by these automated approaches such as the selection of cut-off points [19] or validation of edge detection algorithms and distinguishing artefacts from lesions [20] and reported opposing interpretations of A-scan profiles may suggest that it could be an unreliable indicator of lesion severity [21].

Moreover, fissure caries are often multi-loci. It is most frequently localized in the lower part of the walls of the fissures (61%) whilst 36% had multiple foci at the upper and lower part of the fissure and 13% were positioned above the entrance of the fissure [22]. The angulation and the distance of the area above the entrance of the fissure (slope) and the wall of the fissure, relative to source of the OCT light is substantially different. In view of that, the nature of light attenuation and therefore the detection performance could be affected by whether the foci of the lesion were on the slope of a fissure or at the bottom of wall of a fissure. A recent study concluded that different incidence angle of up to 40° affects significantly the detection of fissure caries [23] with angulation other than 0° showing better detection performance. The development of automated algorithm has so far been developed and investigated on solitary lesions [24,25] and with an incidence angle being 0°. The applicability of these algorithm on fissure caries lesion with multiple loci on the slopes and walls of the fissure is hence unknown. It would also involve more volume of data and potentially require higher computational power and time to analyse the multiple loci.

For a detection method to be successfully translated into the clinical setting, it needs to be relatively economical, does not need to be scanned at multiple axis so as not to be confounded by patient movements, and quick and accurate interpretation of the presence or absence of a non-cavitated lesion. Qualitative assessments are carried out by visually assessing an OCT B-scan to determine the presence of areas of increased backscattered intensity, which is consistent to a caries lesion. This is analogous to the determination of presence of radiolucency of dentine caries lesions in bitewing radiographs. Qualitative assessment of B-scans, although only provides a dichotomous result of presence or absence of caries, it is nevertheless quick and of good practicality. This is especially true in the simultaneous appreciation of the distribution, pattern and dimension of the multiple loci of fissure caries lesions.

However, strong surface specular reflectivity of enamel confounds the reflectivity increase caused by demineralisation and hence produces false positive results. Polarisation-sensitive (PS-)OCT has been shown to be able to eliminate this confounding effect as the perpendicular axis PS-OCT B-scans were found to provide better resolution of the lesion structure including the respective surface zones [26,27]. Cross-polarisation (CP-) OCT on the other hand has been shown to reduce specular reflectance by 20–30 dB and the reflectivity from sound enamel is also suppressed near the tooth surface resulting in higher contrast between sound and demineralised enamel [21].With Swept Source (SS-) and Spectral Domain (SD-) OCT (hereafter to be referred collectively as OCT), techniques such as digital image processing [28], creating an angle up to 45° to the incidence of light [29], use of index matching media [30], systematically excluding combination of depths [31], applying threshold level [26] and a statistical cut-off depth to data [32] are a few examples used to reduce the specular reflection in OCT. Such methods are useful on smooth surface caries lesions with relatively homogeneous demineralisation but are not feasible on occlusal surface with convoluted geometry and multi-loci fissure caries. The confounding effect of surface specular reflection is reflected in the high sensitivity but varied specificity reported in previous studies that involved one rater. Gomez et al. [18] reported high sensitivity (0.98) but poor specificity (0.52) of OCT in detecting fissure caries whilst Shimada et al. [10] reported similar sensitivity of 0.98 but a higher specificity of 0.75. When more than one rater were involved, huge inter-rater kappa range (0.25–0.75)[23] was reported. It is not clear what visual interpretation criteria, if any, was used in these studies and more importantly whether there was any systematic attempt to exclude specular reflection from the interpretation. It is also not clear whether only the wall or slope loci or both of NCFC were considered because it is evident from Park et al's study [23] that the inclusion or exclusion of the wall or slope lesions would affect its detection performance.

Measurement of lesion dimension could be used to monitor progression or regression of caries lesions over time. Remineralisation of enamel caries lesions has been shown to result not only in the decrease of backscattered intensity but also the decrease of the area with observed increased reflectivity [33]. Fried et al. conducted a longitudinal study of simulated-caries lesion using pH cycling model over 1 and 14 days and concluded that depth and severity of lesion is linearly correlated with the square root of demineralisation and PS-OCT is valuable to observe the course of lesion advancement over time [26]. However, the accuracy of the measurement is not known.

Thus, the main objective of our study is to evaluate the detection accuracy of OCT for NCFC when it is assessed in totality and when only the wall or slope loci was assessed using a visual interpretation criteria. The secondary objective was to evaluate the agreement between the measurements of the wall and slope loci of NCFC measured with OCT with that measured with Polarized Light Microscopy (PLM). The null hypothesis is there is no significant difference between PLM and OCT measurements.

2. Materials and methods

2.1. Sample preparation

Fifty-four extracted permanent maxillary and mandibular human premolars were used in this study. Teeth with fluorosis and staining were excluded from the study. The teeth were stored in 1% chloramine solution for 2 weeks to inhibit bacterial growth and in normal saline thereafter. The fissures were cleaned with slurry of pumice with polishing tips with a low speed hand piece and rinsed with water for 10 s to ensure removal of any residuals. The teeth were then sectioned 3 mm below the cemento-enamel junction and mounted in epoxy resin leaving the crowns exposed. In order to ensure equal distribution of NCFC of different stages, ninety preliminary investigation sites with ICDAS code 0, 1, 2 (n = 30 each) were identified using standard ICDAS protocol (http://www.icdas.org/) by two trained and calibrated examiners (EZ and SK).

2.2. OCT imaging of fissure

The premolars were kept moistened, and just before being scanned with OCT, they were air dried for 5 s with a three-in-one syringe. A Swept-source OCT Imaging System (OCS1300SS, Thorlabs Ltd., UK) with emission wavelength centred at 1325 nm and axial and transverse resolution of 9 µm and 11 µm in air, respectively, was used to scan the identified invertigation sites. The Thorlabs OCT capturing software (Swept Source OCT Imaging System Version 2.3.1, Thorlabs) was used to capture the image, configure the OCT settings and guide the light beam. The scanning beam was oriented perpendicular to the fissure and configured to cover an area of 3 mm x 3 mm in the x-y direction and a depth of 3 mm in air, corresponding to 1.85 mm in enamel (refractive index = 1.62). The x-y-z resolution was 1024 × 104 × 512 pixels, respectively. Therefore, a total of 104 OCT cross-sectional scans (B-scans), approximately 30 µm apart, were attained for each investigation site in order to facilitate the identification of a best matching OCT B-scan to the PLM section. The B-scans were captured in logarithmic scale and saved in the Large DR3 colour map of the image capturing software. The brightness and contrast were configured to cover an intensity range between −36 dB and −10 dB.

2.3. Polarized light microscopy (PLM)

Two 180 ± 10 µm thick-serial sections, 200 ± 10 µm apart, were obtained from each of the identified investigation site using the Exakt 300CP Band system (Exakt, Germany). The sections were made in the bucco-lingual direction perpendicular to the fissure using a cutting band of 200 µm thickness with grade D diamonds. No further polishing and finishing was performed after sectioning to avoid affecting the lesions. The section with the most severe lesions of the two was used. The selected sections were then imbibed in water and examined under 4×-magnification. The microscope (Nikon Eclipse 55i, Nikon, Japan) was equipped with an analyzer slide (Nikon C-AS Nikon, Japan), a polariser (Nikon C-TP Nikon, Japan) for first order red compensation, and an integrated digital camera (Nikon DSFI2, Nikon, Japan).

2.4. Final sample selection

From the PLM sections, a final cohort of seventy one investigation sites were selected based on the Ekstrand histology criteria [34] (Table 1), with a distribution of Ekstrand score 0 (n = 21), 1 (n = 25) and 2 (n = 25). The Ekstrand score 1 and 2 were grouped collectively as NCFC for the subsequent analysis. The OCT B-scans that correponded to the selected PLM sections were then identified from the available 104 B-scans, based upon fissure anatomy and cuspal slopes by two examiners (EZ, HPC).

2.5. Interpretation of OCT B-scans and PLM images

2.5.1. Division of fissure

For the interpretation of the OCT B-Scans and PLM images, the fissures were divided into two anatomical sites at the entrance of the fissure, as described first by Fejerskov et al. [35] and later modified by Juhl [22]. The entrance of the fissure (Fig. 1) is defined as the point where its width was 200 µm [22]. In order to facilitate description, the area above the entrance hereafter was termed as slopes (*S*). The limits of the slope was within 500 µm from the entrance of the fissure (Fig. 1) and were labelled on each of the OCT B-scans and PLM images. The area below the entrance of the fissure was termed as walls (*W*) (Fig. 1). Consequently, the lesion foci observed at the slopes were referred as S_L and those observed at the walls referred as W_L (Fig. 1).

The OCT B-scans and PLM images were displayed on a computer

Table 1
Ekstrand histology classification [34].

Score 0	No enamel demineralisation or a narrow surface zone of opacity (edge phenomenon).
Score 1	Enamel demineralisation limited to the outer 50% of the enamel layer.
Score 2	Demineralisation involving between 50% of the enamel and outer third of the dentine.

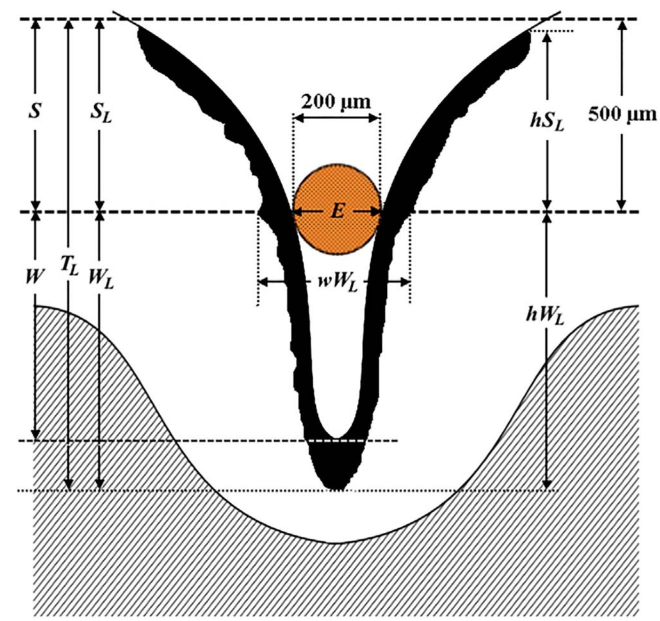

Fig. 1. Illustration of an occlusal fissure showing its sub-divisions [22,35]. Entrance (*E*), slope (*S*), wall (*W*) and its loci; slope loci (S_L), wall loci (W_L), total loci (T_L) and the NCFC dimensions; height of slope loci (hS_L), width of wall loci (wW_L) and height of wall loci (hW_L).

screen and standardised in size, aspect ratio and brightness for evaluation by two trained and calibrated examiners (EZ and MH). Assessment of the fissure for NCFC was performed in separate occasions, for the following sites:

i) Fissure in totality (*T*) (including the slopes and walls).
ii) Slopes (*S*) only.
iii) Walls (*W*) only.

2.5.2. Interpretation criteria for absence and presence of caries

On the PLM images, absence of dark brown and black areas at the investigation sites were considered as sound (Fig. 2a), whereas, the presence of these dark brown and black areas were regarded as carious (Fig. 2b).

On the OCT B-scans, a NCFC is considered to be present when bands of elevated backscattered intensity, in the range of −15 dB to −5 dB, which are sub-surface and diffused in nature (Fig. 2d) were observed. Intensity in the same range which is limited to one to two pixels thick on the surface was NOT considered as carious (Fig. 2c). This intensity range is presented as yellow and red by the *Large DR3* colour map of the Thorlabs OCT capturing software.

2.6. Measurements of lesion dimension

In addition to the above, measurement of the dimension of the NCFC was carried out with PLM and OCT. The measurements were done on the OCT B-scans and PLM images using the Thorlabs OCT software (Swept Source OCT Imaging System Version 2.3.1, Thorlabs, USA) and the Nikon software (NIS- Elements AR 3.2 Nikon Japan), respectively.

The following dimensions were obtained (Fig. 1**)**:

i) Height of slope loci (hS_L): The vertical extent of S_L, within 500 µm from the entrance of the fissure.
ii) Width of wall loci (wW_L): The horizontal extent W_L
iii) Height of wall loci (hW_L): The vertical extent W_L

Two trained and calibrated examiners (EZ and MH) measured the

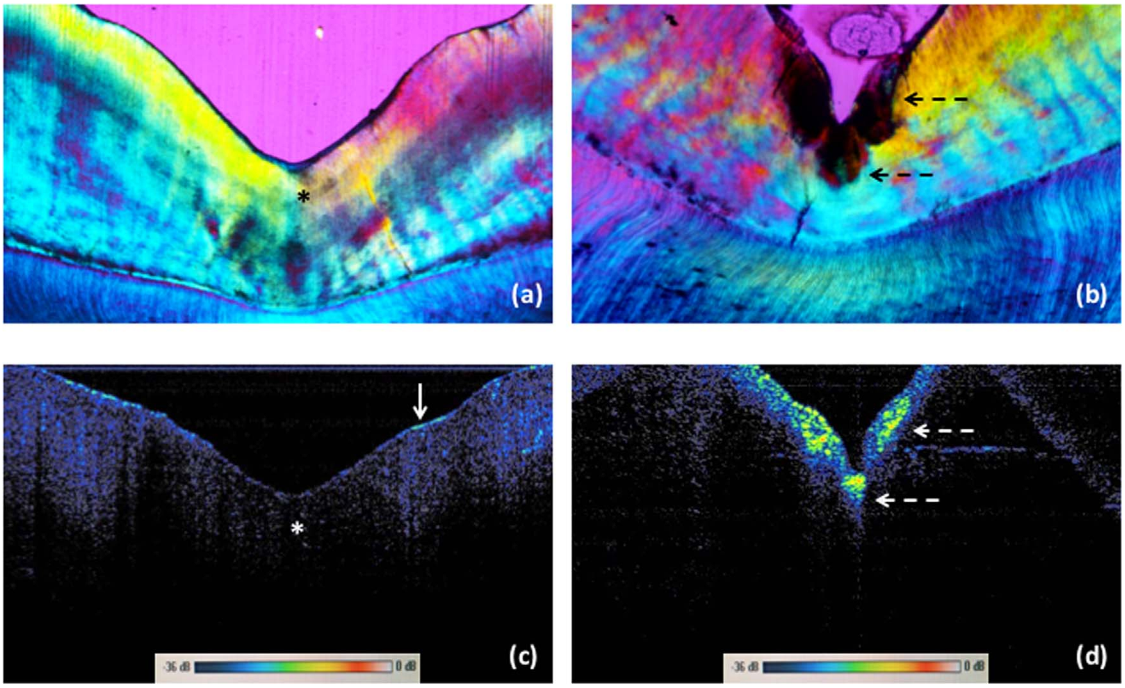

Fig. 2. Interpretation criteria for detection of NCFC with PLM and OCT.
a) PLM image of a sound fissure. There is absence of dark brown and black areas at the investigation site (as indicated by asterisk *); b) PLM image of a NCFC. There are dark brown and black areas (as shown by dashed arrows) at the investigation site; c) Corresponding OCT B-scan of the sound fissure in (a). There is a distinct surface border limited to one to two pixels thick in the yellow/red range (–15 dB to −5 dB) and absence of subsurface and diffused bands of elevated intensity in the yellow/red range (–15 dB to −5 dB) of the color map (as indicated by asterisk *). Specular reflection is shown by the solid arrow; d) Corresponding OCT B-scan of the NCFC in (b). There are presence of subsurface diffused bands of elevated intensity (as shown by dashed arrows) appearing in the yellow/red range (–15 dB to −5 dB) of the colour map.

NCFCs on OCT B-scans and PLM images separately and on two different occasions. For the assessment of level of agreement between the measurements done with OCT and PLM, the measurements of the two examiners were averaged. A consensual measurement was obtained for inter-examiner measurements that differ greater than 50%. The difference of measurements between these two techniques, Δm (PLM measurement − OCT measurement), was calculated for each sample.

2.7. Statistical analysis

Statistical analysis was performed using SPSS (SPSS version 12, IBM, USA). Inter-examiner agreement for the detection of lesions was calculated using Cohen's un-weighted kappa. The detection sensitivity and specificity of OCT for NCFC, as a whole or separately on the slope or wall of the fissure were compared against PLM. For the analysis of sensitivity and specificity, a consensus score was sought in the event of a discrepancy between examiners.

Inter-examiner agreement for the measurement of lesion dimension was calculated using single measure intra-class coefficient (ICC), with a 2-way mixed effect model and consistency type. One-Sample T test was performed to evaluate whether Δm was significantly different from zero. The measurement agreement between OCT and PLM was also evaluated using the Bland-Altman plot. In cases where Δm was significantly different from zero, linear regression was carried out on the Bland-Altman plot to evaluate the existence of bias.

3. Results

3.1. Distribution of the lesions with respect to its anatomical location

The analysis was performed on the final cohort of the 71 investigation sites. Disease prevalence was 70.42%. 74% of the NCFC were found to have both S_L and W_L. The distribution of S_L and W_L of samples with NCFC are as shown in Table 2.

Table 2
Distribution of S_L and W_L of samples with NCFC.

Loci	Ekstrand histological Score 1	Ekstrand histological Score 2	Total
W_L only	7	1	8
W_L and 1 S_L	2	3	5
W_L and 2 S_L	16	21	37

3.2. Detection of lesions

3.2.1. Inter-observer agreement

Inter-observer agreement was used to assess the reliability of the interpretation criteria for OCT and PLM used in this study to detect NCFC. Substantial inter-examiner agreement was found for the detection of NCFC, in totality (T_L) and as separate slope (S_L) and wall (W_L) loci with both OCT and PLM. Un-weighted kappa ranging from 0.82 − > 0.99 and 0.85–0.87 was observed for PLM and OCT respectively (Table 3).

3.2.2. Sensitivity and specificity

Table 4 shows the sensitivities, specificities, positive and negative predictive values and positive and negative likelihood ratios for NCFC detection with OCT, in totality (T_L) and as separate slope (S_L) and wall (W_L) loci. The detection of the lesion as a total lesion (T_L) has the highest sensitivity when compared to detection of S_L or W_L loci separately. On the other hand, detection specificity for T_L and W_L was similarly high whilst that for S_L was the lowest.

3.3. Measurement of lesion dimension

3.3.1. Inter-observer agreement

Good inter-observer agreement was found in the measurement of hS_L, wW_L and hW_L with an ICC ranging from 0.65–0.85 for OCT and

Table 3
Inter-observer agreement for detection of NCFC using OCT and PLM.

Loci	OCT			PLM		
	Percentage agreement	Kappa agreement	P value	Percentage agreement	Kappa agreement	P value
Total loci (T_L)	94%	0.87	< 0.001	> 99%	> 0.99	< 0.001.
Slope loci (S_L)	93%	0.85	< 0.001	92%	0.82	< 0.001
Wall loci (W_L)	94%	0.87	< 0.001	> 99%	> 0.99	< 0.001

0.81–0.98 for PLM respectively (Table 5).

3.3.2. Agreement between OCT and PLM measurements

The mean of Δm, were −0.08 mm, 0.57 mm and 0.03 mm for hS_L, hW_L and wW_L respectively. One-Sample T test showed that Δm for hS_L and hW_L was significantly different from zero ($p < .05$) whilst wW_L was not ($p > .05$) (Table 6). Hence the null hypothesis was rejected for Δm of hS_L and hW_L but not for wW_L.

The Bland-Altman plot for wW_L shows a random spread of Δm around the mean with most values falling within 2 standard deviations (Fig. 3a). The Bland-Altman plot for hS_L (Fig. 3b) also shows a random distribution of Δm around the mean, with the majority falling within 2 standard deviations. However linear regression analysis showed no significant linear relationship between Δm and the mean values of the measurements ($p > .05$). This suggests that there is no proportional bias between the measurements made with PLM and OCT for hS_L and the mean of 0.08 mm is a constant bias. The Bland-Altman plot for hW_L (Fig. 3c) also showed the majority of Δm falling within 2 standard deviations. However, a random distribution was not observed. Linear regression analysis showed significant linear relationship between the Δm and mean values of the measurements ($p < .05$) with a R^2 value of 0.76. This suggests that a proportional bias exist between the measurements of the two techniques for hW_L.

4. Discussion

This study takes a close look at the detection and measurement of NCFC with OCT, with the lesion in its totality and also its slope and wall loci separately, and compares these to those of PLM.

Cavitated lesions were not included in this study because differentiating fissures with cavitated caries from sound ones is a straight forward process. Moreover, the inclusion of cavitated lesions into the sample population of an assessment of detection performance for NCFC can result in over estimation of sensitivity whilst the inclusion of higher number of sound samples could increase the specificity [36]. Therefore, in order to ensure equal distribution of sound and NCFC samples, Ekstrand score 0 (n = 21), 1 (n = 25) and 2 (n = 25) were included in this study. More than one investigation sites were selected from one tooth because the presence of healthy enamel between the investigation sites indicated two independent lesions. All the NCFC (n = 50) in this study were found to have wall loci while 84% was observed to have slope loci on one or both slopes of the fissure (Table 2). Juhl [22] however reported that 80.5% of carious fissure had wall lesions and only 13% have slope lesions. A possible reason for more slope lesions observed in this study could be because Juhl's samples were exclusively maxillary premolar where the angulation of its cusp slopes are steeper than those of mandibular premolars. This study assessed the detection accuracy of visual assessment OCT B-scans for NCFC in totality and either on the slope or wall of the fissure because the pattern of demineralisation in NCFC is not homogenous and signs of early demineralisation do not always involve the whole length of the fissure and or the slope of the fissure concurrently [37]. It may occur either independently on the slope or wall of a fissure and then coalesce on both sites of a fissure [22]. The division of NCFC into the slope and wall loci was done at the fissure entrance width of 200 μm, as previously described by Juhl [22]. Clinically, this could be described as the point where the access of a dental explorer to a fissure is being blocked by the walls of the fissure [35].

Previous studies that evaluated the detection accuracy of visual assessment OCT B-scans for fissure caries [10,18,38] included cavitated lesions in their sampling and used a four-point index to stage fissure caries from the non-cavitated to cavitated ones. However, no interpretation criteria were described and employed to characterise the increased intensity of demineralised enamel and most importantly to differentiate it from the increased reflectivity caused by specular reflection. The range of intensity due to specular reflection is similar to the intensity range of demineralised enamel, and thus confounds the observation of NCFC, especially the slope loci and potentially give rise to false positive results. Gomez et al. [18] acknowledged that in the absence of interpretation criteria, the visual assessment method suffered from subjectivity. The interpretation criteria for NCFC developed and used in this study had good reliability, as attested by the inter-observer kappa score of 0.85 to 0.87 (Table 3). The interpretation criteria were developed based upon the location, thickness and pattern of the intensity range of −15 db to −5 db, presented on the colour scale mentioned above (Fig. 2c).

We found that using visual assessment of OCT B-scan, the detection of NCFC in totality had excellent sensitivity (0.98) and specificity (0.95). The sensitivity observed in this study concurred with that of Shimada et al. [10] and Gomez et al. [18] where they reported sensitivity of 0.98 and 0.95 respectively for the detection of caries lesion that was described as having "*Demineralisation limited to enamel only but loss of enamel surface (cavitation) had not occurred*". Unanimous high sensitivity across these two previous studies and our study indicates that a true NCFC will almost always (sensitivity approximates 1) be picked up during the visual assessment of OCT B-scans and there will be almost always no false negative results. Specificity however, as reported by Shimada et al. [10] and Gomez et al. [18] was 0.75 and 0.39 respectively. The higher specificity observed by Shimada et al. when compared to Gomez et al.'s might be because Shimada et al.'s B-scan visual assessment results were the consensus of three examiners' whilst only one examiner was involved in Gomez et al.'s study. When compared to

Table 4
Sensitivity and specificity for detection of NCFC using OCT.

Loci	Sensitivity	Specificity	Positive predictive value (PPV) (%)	Negative predictive value (NPV) (%)	Positive Likelihood ratio (LR +)	Negative Likelihood ratio (LR −)
Total loci (T_L)	0.98	0.95	98	95	21	0.02
Slope loci (S_L)	0.95	0.90	93	93	9.21	0.05
Wall loci (W_L)	0.94	0.95	98	87	20	0.06

Table 5
Inter-observer agreement for dimension measurements of NCFC using OCT and PLM.

Loci	OCT				PLM			
	Intra class correlation (consistency)	P value	Lower bound 95% CI	Upper bound 95% CI	Intra class correlation (consistency)	P value	Lower bound 95% CI	Upper bound 95% CI
Height of slope loci (hS_L)	0.65	< 0.001	0.501	0.767	0.92	< 0.001	0.880	0.951
Width of wall loci (wW_L)	0.82	< 0.001	0.713	0.901	0.81	< 0.001	0.686	0.891
Height of wall loci (hW_L)	0.85	< 0.001	0.746	0.914	0.98	< 0.001	0.974	0.992

Table 6
One-Sample T test and linear regression analysis for dimension measurements of NCFC between OCT and PLM.

	hS_L	hW_L	wW_L
Δm 95% CI (mm)	−0.08 (−0.13 to −0.04)	0.57 (0.46–0.68)	0.03 (−0.01–0.06)
P value (One-Sample T test)	0.001	< 0.001	0.178
P value (linear regression analysis)	0.23	< 0.001	NA
R^2 value (linear regression analysis)	0.05	0.76	NA
Standardized coefficient of regression line	0.21	0.87	NA

Shimada et al's study, the detection specificity was enhanced further in our study (0.95), most likely due to the use of interpretation criteria to differentiate the increased backscattered intensity due to specular reflection from that is due to demineralisation. To a lesser extent, the detection specificity in this study could have also been enhanced by three-dimensional OCT scans of investigation sites that had facilitated the selection of OCT B-scans that best matched the PLM image and also by the use of a colour scale that enhanced the contrast of the range of intensity of demineralisation. When comparing the detection ability of OCT for NCFC in totality or by the wall or slope loci separately, there were similar high sensitivity (0.98, 0.94 and 0.95 respectively), i.e. very few lesions are missed in both cases. However, there was a bigger disparity between the specificity for the detection of wall and slope loci (0.95 and 0.90 respectively), i.e. there is a higher likelihood of false slope lesions identified compared to wall lesions. This disparity could be because slope lesions, due to its position and inclination, are confounded by specular reflections more than wall lesions. Therefore the differentiation between specular reflection and increased subsurface backscattered intensity signals maybe be difficult in some cases [39].

In this study we also studied the agreement between the measurement made with OCT and PLM of the slope and wall loci of NCFC. OCT and PLM width measurements of wall loci (wW_L) was found to be not statistically different from each other. This indicates that OCT B-scans could be used in place of PLM when the width of the wall loci of NCFC is to be measured.

OCT and PLM measurements of the height dimensions, hS_L and hW_L however was found to be statistically different from each other. OCT measurements for hS_L were found to be constantly 0.08 mm bigger in average than PLM measurements. This could be due to a calibration offset in the optical properties of the enamel due to refraction index used. Hariri and colleagues had observed change in the refractive index from 1.52 to 1.63 when the mineral content decreased from 50% to 87% in enamel respectively [40]. Most of the difference between OCT and PLM measurements was randomly distributed within the 95% limits of agreement, i.e. within two standard deviations. As the difference of 0.08 mm does not increase with the dimension of the slope lesion (constant bias), and is not clinically significant or discernible and not likely to affect treatment decisions, it could be considered clinically acceptable to use height measurements of slope loci to monitor NCFC. On the other hand, height measurements of wall loci (hW_L) or sometimes termed lesion depth of OCT was found to be 0.57 mm smaller in average than PLM measurements. Although most of the difference between the two measurements lies within two standard deviations (Fig. 3c), a proportional bias was observed and it is linearly correlated with the size of the lesion. An average underestimation of 0.57 mm of lesion depth is paramount clinical significance especially when the distance between the base of a fissure to the enamel-dentinal junction is most of the time less than 1 mm. This could result in grave clinical consequence under-management of a NCFC. Thus OCT B-Scans should not be used to measure height of wall loci (hW_L) or lesion depth of

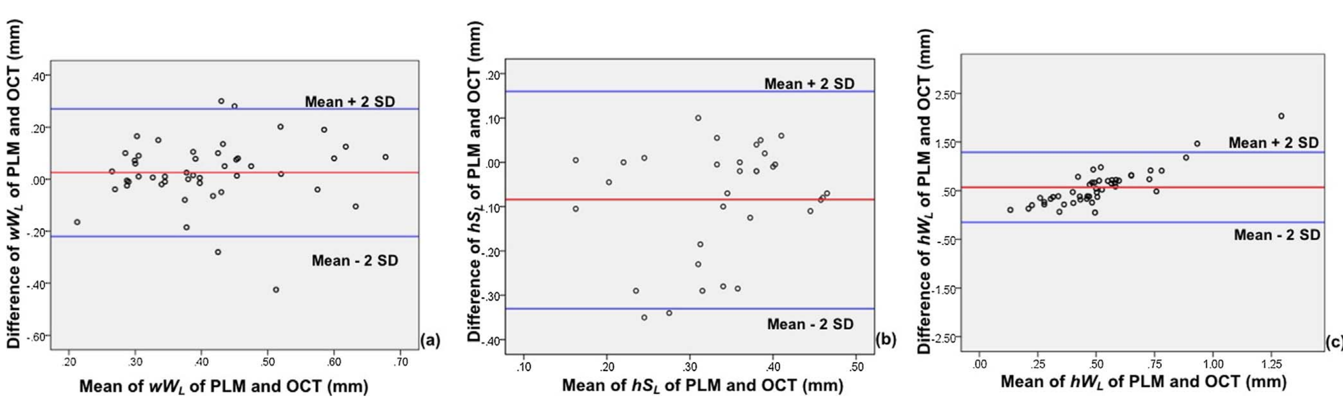

Fig. 3. Bland Altman plots for wW_L, hS_L and hW_L measured with OCT and PLM.
The red line of the three graphs indicates the mean of difference between PLM and OCT measurements and the upper and lower blue lines represents ± 2 standard deviations. (a) and (b) - The Δm of wW_L and hS_L are spread evenly around the mean (0.03 mm and −0.08 mm respectively), with most values falling within 2 standard deviations, suggesting no proportional bias between them and their respective mean value; (c) - The spread of Δm of hW_L is also within 2 standard deviations of the mean (0.57 mm) but a significant linear relationship is observed, indicating presence of proportional bias.

NCFC.

5. Conclusion

Unanimous high sensitivity observed in this and previous studies [10,18] indicates that visual assessment of OCT B-scans is useful to rule out NCFC. However, variable specificity reported from previous studies [10,18] contradicts with the high specificity observed in this study. Our study indicates that the reliability of visual assessment of OCT B-scans to detect NCFC may be enhanced by the use of interpretation criteria that differentiate increased backscattered intensity due to specular reflection from that due to demineralisation. Detection reliability could also be increased by the use of a colour scale that increased the contrast of the range of backscattered intensity of demineralisation. Detection sensitivity and specificity were not affected whether NCFC were assessed in totality or by wall or slope loci separately. For the monitoring of NCFC dimensions with OCT, measurements should be confined to the width measurements of wall loci and/or height measurements of slope loci whilst the height measurements of wall loci, or lesion depth, should be avoided. Although there are limitations in using OCT to measure the height of wall loci, future work could explore correlation between the width and height of the wall loci, which could potentially be used indirectly as a surrogate to measure the height of wall loci.

Acknowledgement

This study was supported by High Impact Research MoE Grant UM.C/625/1/HIR/MoE/DENT/11 from the Ministry of Education Malaysia.

The authors wish to acknowledge the contribution of Associate Professor Karuthan Chinna in statistical analysis consultation, Dr Madiha Habib (MH) as the second examiner in assessing the OCT B-scans and PLM images, Dr Saad Khan (SK) in the initial identification of samples with NCFC and Dr Ali Dabbagh in the illustration of Fig. 1.

References

[1] W. Marcenes, N.J. Kassebaum, E. Bernabe, A. Flaxman, M. Naghavi, A. Lopez, C.J. Murray, Global burden of oral conditions in 1990–2010: a systematic analysis, J. Dent. Res. 92 (7) (2013) 592–597.

[2] L.W. Ripa, Occlusal sealing: rationale of the technique and historical review, J. Am. Soc. Prev. Dent. 3 (1) (1973) 32–39.

[3] J.A. Brunelle, Oral Health of United States Children. The National Survey of Dental Caries in US Schoolchildren: 1986-87 Findings. NIH Pub No 89–2247, US Department of Health and Human Services, Washington, DC, 1989.

[4] A.I. Garcia, Caries incidence and costs of prevention programs, J. Public Health Dent. 49 (5 Spec No) (1989) 259–271.

[5] J. Kuhnisch, K.R. Ekstrand, I. Pretty, S. Twetman, C. van Loveren, S. Gizani, M. Spyridonos Loizidou, Best clinical practice guidance for management of early caries lesions in children and young adults: an EAPD policy document, Eur. Arch. Paediatr. Dent. 17 (1) (2016) 3–12.

[6] C.L. Longbottom, M.C. Huysmans, N.B. Pitts, M. Fontana, Glossary of key terms, Monogr. Oral Sci. 21 (2009) 209–216.

[7] J. Gomez, M. Tellez, I.A. Pretty, R.P. Ellwood, A.I. Ismail, Non-cavitated carious lesions detection methods: a systematic review, Community Dent. Oral Epidemiol. 41 (1) (2013) 54–66.

[8] M.B. Diniz, J.A. Rodrigues, I. Hug, C. Cordeiro Rde, A. Lussi, Reproducibility and accuracy of the ICDAS-II for occlusal caries detection, Community Dent. Oral Epidemiol. 37 (5) (2009) 399–404.

[9] A. Jablonski-Momeni, V. Stachniss, D.N. Ricketts, M. Heinzel-Gutenbrunner, K. Pieper, Reproducibility and accuracy of the ICDAS-II for detection of occlusal caries in vitro, Caries Res. 42 (2) (2008) 79–87.

[10] Y. Shimada, A. Sadr, M.F. Burrow, J. Tagami, N. Ozawa, Y. Sumi, Validation of swept-source optical coherence tomography (SS-OCT) for the diagnosis of occlusal caries, J. Dent. 38 (8) (2010) 655–665.

[11] M.M. Braga, L.B. Oliveira, G.A. Bonini, M. Bonecker, F.M. Mendes, Feasibility of the International Caries Detection and Assessment System (ICDAS-II) in epidemiological surveys and comparability with standard World Health Organization criteria, Caries Res. 43 (4) (2009) 245–249.

[12] N.B. Pitts, J.W. Stamm, International consensus workshop on caries clinical trials (ICW -CCT)–final consensus statements: agreeing where the evidence leads, J. Dent. Res. (2004) C125–C128 83 Spec No C.

[13] A.C. Pereira, H. Eggertsson, E.A. Martinez-Mier, F.L. Mialhe, G.J. Eckert, D.T. Zero, Validity of caries detection on occlusal surfaces and treatment decisions based on results from multiple caries-detection methods, Eur. J. Oral Sci. 117 (1) (2009) 51–57.

[14] J. Brinkman, J.J. ten Bosch, P.C. Borsboom, Optical quantitation of natural caries in smooth surfaces of extracted teeth, Caries Res. 22 (5) (1988) 257–262.

[15] C.L. Darling, G.D. Huynh, D. Fried, Light scattering properties of natural and artificially demineralized dental enamelat 1310 nm, J. Biomed. Opt. 11 (3) (2006) 34023.

[16] J.S. Holtzman, J. Ballantine, M. Fontana, A. Wang, A. Calantog, E. Benavides, C. Gonzalez-Cabezas, Z.P. Chen, P. Wilder-Smith, Assessment of early occlusal caries pre- and post-Sealant application-An imaging approach, Lasers Surg. Med. 46 (6) (2014) 499–507.

[17] T. Louie, C. Lee, D. Hsu, K. Hirasuna, S. Manesh, M. Staninec, C.L. Darling, D. Fried, Clinical assessment of early tooth demineralization using polarization sensitive optical coherence tomography, Lasers Surg. Med. 42 (10) (2010) 738–745.

[18] J. Gomez, C. Zakian, S. Salsone, S.C. Pinto, A. Taylor, I.A. Pretty, R. Ellwood, In vitro performance of different methods in detecting occlusal caries lesions, J. Dent. 41 (2) (2013) 180–186.

[19] A.M. Can, C.L. Darling, C. Ho, D. Fried, Non-destructive assessment of inhibition of demineralization in dental enamel irradiated by a lambda = 9.3-microm CO2 laser at ablative irradiation intensities with PS-OCT, Lasers Surg. Med. 40 (5) (2008) 342–349.

[20] M.H. Le, C.L. Darling, D. Fried, Methods for calculating the severity of demineralization on tooth surfaces from PS-OCT scans, Proc. Soc. Photo-Opt. Instrum. 7162 (2009).

[21] K.H. Chan, A.C. Chan, W.A. Fried, J.C. Simon, C.L. Darling, D. Fried, Use of 2D images of depth and integrated reflectivity to represent the severity of demineralization in cross-polarization optical coherence tomography, J. Biophotonics 8 (1-2) (2015) 36–45.

[22] M. Juhl, Localization of carious lesions in occlusal pits and fissures of human premolars, Scand. J. Dent. Res. 91 (4) (1983) 251–255.

[23] K.J. Park, R. Haak, D. Ziebolz, F. Krause, H. Schneider, OCT assessment of non-cavitated occlusal carious lesions by variation of incidence angle of probe light and refractive index matching, J. Dent. 62 (2017) 31–35.

[24] T. Ibusuki, Y. Kitasako, A. Sadr, Y. Shimada, Y. Sumi, J. Tagami, Observation of white spot lesions using swept source optical coherence tomography (SS-OCT): in vitro and in vivo study, Dent. Mater. J. 34 (4) (2015) 545–552.

[25] P. Ngaotheppitak, C.L. Darling, D. Fried, J. Bush, S. Bell, PS-OCT of occlusal and interproximal caries lesions viewed from occlusal surfaces, Lasers Dent. XII 6137 (2006) L1370.

[26] D. Fried, J. Xie, S. Shafi, J.D. Featherstone, T.M. Breunig, C. Le, Imaging caries lesions and lesion progression with polarization sensitive optical coherence tomography, J. Biomed. Opt. 7 (4) (2002) 618–627.

[27] P. Ngaotheppitak, C.L. Darling, D. Fried, Measurement of the severity of natural smooth surface (interproximal) caries lesions with polarization sensitive optical coherence tomography, Lasers Surg. Med. 37 (1) (2005) 78–88.

[28] D.C. Adler, T.H. Ko, J.G. Fujimoto, Speckle reduction in optical coherence tomography images by use of a spatially adaptive wavelet filter, Opt. Lett. 29 (24) (2004) 2878–2880.

[29] E. Rakhmatullina, A. Bossen, C. Hoschele, X. Wang, B. Beyeler, C. Meier, A. Lussi, Application of the specular and diffuse reflection analysis for in vitro diagnostics of dental erosion: correlation with enamel softening, roughness, and calcium release, J. Biomed. Opt. 16 (10) (2011) 107002.

[30] Y. Natsume, S. Nakashima, A. Sadr, Y. Shimada, J. Tagami, Y. Sumi, Estimation of lesion progress in artificial root caries by swept source optical coherence tomography in comparison to transverse microradiography, J. Biomed. Opt. 16 (7) (2011) 071408.

[31] B.T. Amaechi, A. Podoleanu, S.M. Higham, D.A. Jackson, Correlation of quantitative light-induced fluorescence and optical coherence tomography applied for detection and quantification of early dental caries, J. Biomed. Opt. 8 (4) (2003) 642–647.

[32] H.P. Chew, C.M. Zakian, I.A. Pretty, R.P. Ellwood, Measuring initial enamel erosion with quantitative light-induced fluorescence and optical coherence tomography: an in vitro validation study, Caries Res. 48 (3) (2014) 254–262.

[33] R.S. Jones, D. Fried, Remineralization of enamel caries can decrease optical reflectivity, J. Dent. Res. 85 (9) (2006) 804–808.

[34] K.R. Ekstrand, D.N. Ricketts, E.A. Kidd, Reproducibility and accuracy of three methods for assessment of demineralization depth of the occlusal surface: an in vitro examination, Caries Res. 31 (3) (1997) 224–231.

[35] O. Fejerskov, B. Melsen, T. Karring, Morphometric analysis of occlusal fissures in human premolars, Scand. J. Dent. Res. 81 (7) (1973) 505–509.

[36] E.H. Verdonschot, A. Wenzel, E.M. Bronkhorst, Assessment of diagnostic accuracy in caries detection: an analysis of two methods, Community Dent. Oral Epidemiol. 21 (4) (1993) 203–208.

[37] K.G. Konig, Dental morphology in relation to caries resistance with special reference to fissures as susceptible areas, J. Dent. Res. 2 (1963) 461–476.

[38] Y. Nakajima, Y. Shimada, A. Sadr, I. Wada, M. Miyashin, Y. Takagi, J. Tagami, Y. Sumi, Detection of occlusal caries in primary teeth using swept source optical coherence tomography, J. Biomed. Opt. 19 (1) (2014).

[39] R.S. Jones, C.L. Darling, J.D. Featherstone, D. Fried, Imaging artificial caries on the occlusal surfaces with polarization-sensitive optical coherence tomography, Caries Res. 40 (2) (2006) 81–89.

[40] I. Hariri, A. Sadr, S. Nakashima, Y. Shimada, J. Tagami, Y. Sumi, Estimation of the enamel and dentin mineral content from the refractive index, Caries Res. 47 (1) (2013) 18–26.